PLOS GENETICS

RESEARCH ARTICLE

The VIL gene *CRAWLING ELEPHANT* controls maturation and differentiation in tomato via polycomb silencing

Ido Shwartz[1], Chen Yahav[1], Neta Kovetz[1], Matan Levy[1], Alon Israeli[1], Maya Bar[1¤a], Katherine L. Duval[2¤b], Ellen G. Krall[2], Naama Teboul[1], José M. Jiménez-Gómez[3,4,5], Roger B. Deal[2]*, Naomi Ori[1]*

1 Institute of Plant Sciences and Genetics in Agriculture, The Robert H. Smith Faculty of Agriculture, Food and Environment, The Hebrew University of Jerusalem, Rehovot, Israel, **2** Department of Biology, O. Wayne Rollins Research Center, Emory University, Atlanta, Georgia, United States of America, **3** Department of Plant Breeding and Genetics, Max Planck Institute for Plant Breeding Research, Cologne, Germany, **4** Institut Jean-Pierre Bourgin, INRAE, AgroParisTech, Université Paris-Saclay, Versailles, France, **5** Centro de Biotecnología y Genómica de Plantas (CBGP), Universidad Politécnica de Madrid (UPM)—Instituto Nacional de Investigación y Tecnología Agraria y Alimentaria (INIA-CSIC), Pozuelo de Alarcón, Madrid, Spain

¤a Current address: Department of Plant Pathology and Weed Research, ARO, Volcani Center, Bet Dagan, Israel
¤b Current address: Department of Genetics, University of Georgia, Athens, Georgia, United States of America
* roger.deal@emory.edu (RD); naomi.ori@mail.huji.ac.il (NO)

Citation: Shwartz I, Yahav C, Kovetz N, Levy M, Israeli A, Bar M, et al. (2022) The VIL gene *CRAWLING ELEPHANT* controls maturation and differentiation in tomato via polycomb silencing. PLoS Genet 18(3): e1009633. https://doi.org/10.1371/journal.pgen.1009633

Editor: Ortrun Mittelsten Scheid, Gregor Mendel Institute of Molecular Plant Biology, AUSTRIA

Received: May 27, 2021

Accepted: February 22, 2022

Published: March 7, 2022

Data Availability Statement: Most relevant data are within the manuscript and its Supporting Information files. RNAseq reads used for mapping crel mutantsare available at https://www.ncbi.nlm.nih.gov/sra under project numbers PRJNA347502 (M82) and PRJNA723668 (crel-2 and crel-2). All shoot apex ChIP-seq and RNA-seq datasets have been deposited to the NCBI GEO database and are available under accession number GSE174416.

Funding: This work was supported by grants from the United States – Israel Binational Science

Abstract

VERNALIZATION INSENSITIVE 3-LIKE (VIL) proteins are PHD-finger proteins that recruit the repressor complex Polycomb Repressive Complex 2 (PRC2) to the promoters of target genes. Most known VIL targets are flowering repressor genes. Here, we show that the tomato VIL gene *CRAWLING ELEPHANT* (*CREL*) promotes differentiation throughout plant development by facilitating the trimethylation of Histone H3 on lysine 27 (H3K27me3). We identified the *crel* mutant in a screen for suppressors of the simple-leaf phenotype of *entire* (*e*), a mutant in the AUX/IAA gene ENTIRE/SlIAA9, involved in compound-leaf development in tomato. *crel* mutants have increased leaf complexity, and suppress the ectopic blade growth of *e* mutants. In addition, *crel* mutants are late flowering, and have delayed and aberrant stem, root and flower development. Consistent with a role for CREL in recruiting PRC2, *crel* mutants show drastically reduced H3K27me3 enrichment at approximately half of the 14,789 sites enriched in wild-type plants, along with upregulation of many underlying genes. Interestingly, this reduction in H3K27me3 across the genome in *crel* is also associated with gains in H3K27me3 at a smaller number of sites that normally have modest levels of the mark in wild-type plants, suggesting that PRC2 activity is no longer limiting in the absence of CREL. Our results uncover a wide role for CREL in plant and organ differentiation in tomato and suggest that CREL is required for targeting PRC2 activity to, and thus silencing, a specific subset of polycomb targets.

Foundation (BSF, 2015093) to N.O and R.B.D., German-Israel Project Cooperation Foundation (OR309/1-1;FE552/12-1) to N.O. and J.M.J.-and from the U.S. – Israel Binational Agricultural Research and Development Fund (IS4531-12(c) and IS5103-18R) and the Israel Science Foundation (grants number 2407-18 and 248-19) to NO. AI thanks the Azrieli Foundation for the award of an Azrieli fellowship. E.G.K. was supported by NIH training grant 5T32GM008490. The funders had no role in study design, data collection and analysis, decision to publish, or preparation of the manuscript.

Competing interests: The authors have declared that no competing interests exist.

Author summary

Plants form organs continuously throughout their lives, and the number and shape of their organs is determined in a flexible manner according to the internal and external circumstances. Alongside this flexibility, plants maintain basic developmental programs to ensure proper functioning. Among the ways by which plants achieve flexible development is by tuning the pace of their maturation and differentiation, at both the plant and organ levels. One of the ways plants regulate the rate of maturation and differentiation is by changing gene expression. Here, we identified a gene that promotes plant and organ maturation and differentiation. This gene, *CRAWLING ELEPHANT* (*CREL*) acts by bringing a repressing complex to target genes. We show the importance of CREL in multiple developmental processes and in the expression of multiple genes throughout the tomato genome.

Introduction

Polycomb Repressive Complex 2 (PRC2) is a conserved complex that represses gene expression by trimethylating lysine 27 of histone H3 proteins (H3K27me3)[1–3]. PRC2 activity counteracts, and is counteracted by, the transcription-promoting functions of trithorax-group proteins [4]. The core PRC2 is composed of 4 subunits. In plants, some of these subunits are encoded by small gene families, allowing the formation of multiple, distinct complexes. Different plant PRC2 complexes have been shown to regulate specific developmental processes such as endosperm development, flowering time and flower development [2,3]. As PRC2 complexes do not have DNA binding domains, they are recruited to target loci by interacting proteins [2,5–10]. One of the most characterized PRC2-regulated processes in Arabidopsis is the induction of flowering in response to prolonged cold, termed vernalization. In response to vernalization, PRC2 promotes flowering by silencing the flowering inhibitor FLC. The vernalization-specific VRN-PRC2 complex is recruited to FLC by complexing with PHD proteins from the VERNALIZATION INSENSITIVE 3-LIKE (VIL) family [7,11–13]. In Arabidopsis, the VIL family consists of 4 members, including VIN3 and VRN5. Vernalization induces VIN3 expression, while VRN5 is expressed constitutively. VIL proteins also repress additional members of the FLC family during vernalization, and VRN5 and VIL2 are also involved in other flowering pathways [7,11,14,15].

VIL proteins have been identified from several plant species [16–25]. They have been shown to promote flowering in all tested species, including species that do not have an FLC ortholog and/or do not respond to vernalization. In rice, the *OsLF* and *OsLFL1* genes encode transcription factors that inhibit flowering and have been identified as VIL targets [18,20]. A VIN3 ortholog has also been identified in tomato [24]. While the vast majority of research on VIL proteins concerned their involvement in flowering induction, several studies reported additional developmental effects. For example, Arabidopsis *vrn5* mutants had increased leaf curling, increased numbers of petals, and distorted siliques [13]. In rice, *leaf inclination2* (*lc2*) mutants had an altered leaf angle, curled leaves and severe sterility, and other rice VIL genes were found to affect spikelet development, branching and grain yield [16,17,19,26]. Silencing the *Brachypodium distachyon BdVIL4*, which is similar to *VIN3*, led to increased branching [21]. Pepper *cavil1* mutants affect leaf development, apical dominance and branching [25]. However, the knowledge about the involvement of VIL proteins in these and other developmental processes is limited, and their role in compound-leaf development has not been explored. In addition, it is not clear whether VIL proteins recruit PRC2 mainly to targets

involved in the induction to flowering or whether they have broader roles in plant development.

Tomato plants have compound leaves, which are composed of multiple leaflets [27]. The elaboration of compound leaves depends on slow maturation of the developing leaf, which enables an extended organogenesis activity at the leaf margin, during which leaflets are formed [28–32]. Leaflets are formed by differential growth at the leaf margin, where regions of blade growth are separated by intercalary regions of growth inhibition [33]. Auxin has been shown to promote growth and its response is inhibited in the intercalary domains [34–40]. Mutations in the tomato gene *SlIAA9/ENTIRE* (*E*), encoding an auxin-response inhibitor from the Aux/IAA family that specifies the intercalary domain, result in simplified leaves due to ectopic blade growth in the intercalary domain [34,41,42].

Here, a screen for suppressors of the *e* simple-leaf phenotype identified the *crawling elephant* (*crel*) mutant, which substantially suppresses the ectopic blade growth of *e*. We found *CREL* to encode a tomato VIL gene, related to Arabidopsis *VIL1/VRN5*. *crel* mutants affect many aspects of tomato development, including plant and organ maturation. Comparison of H3K27me3 modifications between wild type and *crel* plants showed that CREL is required for H3K27me3 deposition at approximately half of the H3K27me3-enriched sites found in wild-type plants. Therefore, CREL promotes maturation throughout the plant life by promoting selective deposition of H3K27me3 and gene silencing at a subset of PRC2 targets.

Results

crawling elephant (*crel*) mutants suppress *entire* (*e*) and have very compound leaves

entire (*e*) mutants, mutated in a tomato Aux/IAA gene, have simplified leaves in comparison to the wild-type compound leaves [34,40,42,43] (Fig 1A and 1B). To identify genes that are involved in compound-leaf development, we generated an Ethyl Methane Sulfonate (EMS) mutant population in the background of *e*, and screened for suppressors of the *e* simplified leaf phenotype. This screen identified the *crawling elephant-1* (*crel-1*) mutant as a strong *e* suppressor. *e crel-1* double mutants had distinct, clearly separate primary leaflets, and occasionally had secondary leaflets, in contrast to the mostly entire leaf shape of single *e* mutants (Fig 1A–1C). To characterize the unique *crel-1* phenotype, we backcrossed *crel-1* to the parental line (*Solanum lycopersicum* M82), and identified single *crel-1* F2 individuals (Fig 1D). Leaves of single *crel-1* mutants were much more compound than wild-type leaves, with a similar number of primary leaflets but many more secondary leaflets than the wild type. In contrast to wild type-leaves, *crel-1* leaves also had tertiary leaflets (Fig 1A, 1D, 1J and 1K). Therefore, *crel* mutants suppress the *e* simplified-leaf phenotype, and form many more leaflets in both the wild type and the *e* backgrounds. Interestingly, previously identified *e* suppressors such as *slmp* and *slarf19a,b* had a reduced number of leaflets in the respective single mutants [39].

We identified several additional *crel* alleles from the Menda EMS and fast neutron mutant population [44], in the M82 background, and confirmed allelism by complementation tests. The alleles showed a range of phenotypic severities, including a diverse increase in leaflet number (Fig 1E–1H, 1J and 1K). Similar to *crel-1*, *crel-2* also suppressed the *e* simplified leaf phenotype (S1A–S1D Fig).

CREL acts during relatively late stages of leaf development

To investigate the timing of the effect of *crel* mutants on leaf development, we compared leaf development between wild type and *crel-1* plants. Early stages of leaf development were very

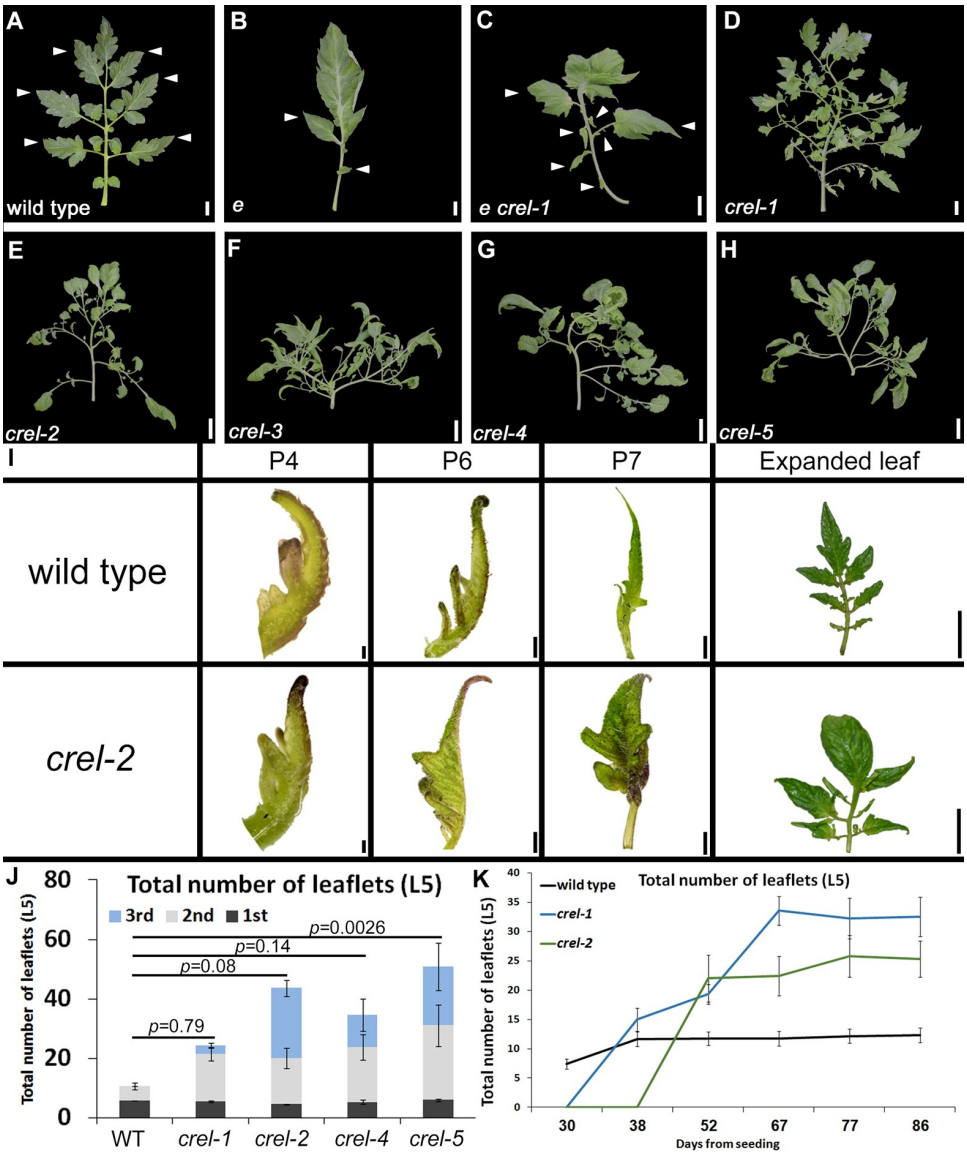

Fig 1. Mutating *crel* suppresses the *e* simple leaf phenotype and produces very compound leaves. (A-H) Mature 5th leaves of the indicated genotypes. A-C suppression of *e* by *crel-1*; D-H: leaves of 5 different *crel* alleles. Scale bars: 2cm. (I) Early leaf development in the fifth leaf of wild type and *crel-2*. P4- P7 designate the developmental stages, where P4 is the forth youngest leaf primordium. Scale bars: 0.1 mm (P4), 0.5 mm (P6), 2 mm (P7), 2 cm (expanded leaf). (J) Quantification of the number of leaflets in a mature 5th leaf of the indicated *crel* alleles, compared to the wild type. 1st, 2nd and 3rd represent primary, secondary and tertiary leaflets, respectivley, where primary leaflets arise from the rachis, secondary leaflets arise from primary leaflets etc. (K) Leaflet production over time by the fifth leaf) L5) of the indicated genotypes.

https://doi.org/10.1371/journal.pgen.1009633.g001

similar between wild type and *crel-1* plants when similar developmental stages were compared, although the terminal leaflet expanded earlier in *crel-1* (Fig 1I). However, the rate of leaf and leaflet initiation was much slower in *crel-1* mutants than in the wild type (S1E Fig). At later stages of leaf development, when wild type leaves stopped generating new leaflets, *crel-1* and *crel-2* leaves continued to form leaflets more than a month later (Fig 1K). Therefore, *crel* leaves develop slower than the wild type, and while the terminal leaflet appears to differentiate early, overall leaf differentiation is substantially delayed in *crel* mutants.

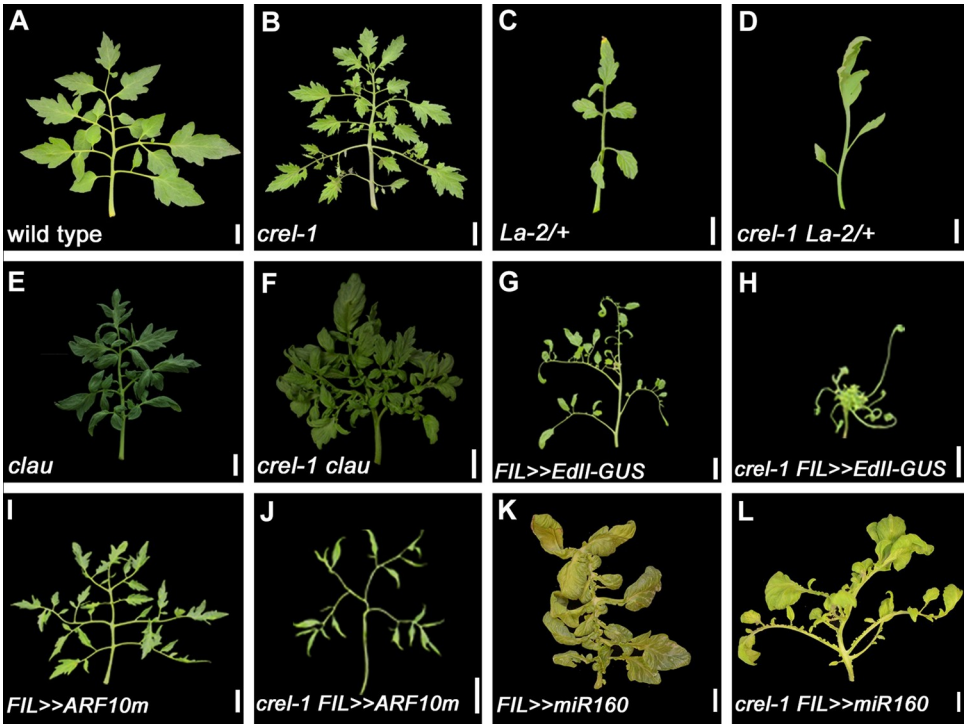

Fig 2. CREL acts relatively late in leaf development to promote differentiation and blade growth. (A-F, I, J) Mature 5th leaves. (K,L) Mature 9th leaves. (G, H) whole plants. Scale bars: 2cm. *FIL>>*gene refers to genotypes generated by the LhG4-OP transactivation system, where the gene is expressed in the *FIL* expression domain. The *FIL* promoter is expressed in leaf primordia [52]; *EdII-GUS* is a stabilized form of *E* fused to the GUS reporter; *ARF10m* is a mutant form of ARF10 that is mutated in the miR160 binding site. A-D—epistasis of *La-2/+*, in which differentiation is accelerated, over *crel*. E, F—enhancment of *crel* by *clau*, in which differentiation is delayed. G-J–enhancment of genotypes with narrow leaves due to reduced auxin response by *crel*. K, L–suppression of the ectopic blade growth of *FIL>>miR160* by *crel*, similar to the effect on *e*.

https://doi.org/10.1371/journal.pgen.1009633.g002

To further characterize this effect of *crel* on leaf development, and understand the timing and developmental context of CREL action, we analyzed its genetic interaction with mutants that affect the developmental window of leaflet morphogenesis. Leaflets are formed during the morphogenesis stage of leaf development, which follows leaf initiation and precedes leaf expansion and differentiation [27,28,45,46]. The elaboration of compound leaves depends on an extended morphogenesis stage. The CIN-TCP transcription factor LANCEOLATE (LA) and the MYB transcription factor CLAUSA (CLAU) promote maturation and differentiation and thereby restrict the morphogenetic window [29,47–50]. *La-2* is a semi-dominant mutant in which *LA* is expressed precociously due to a mutation in the miR319 binding site. This accelerates leaf differentiation and leads to a simple leaf form (Fig 2A and 2C). *La-2* was epistatic to *crel-1* (Fig 2B–2D), indicating that the morphogenetic window in *La-2* is terminated before the timing of CREL action, in agreement with the relatively early effect of *LA* and late effect of *CREL* on leaf development. Leaves of loss-of-function *clau* mutants have an extended morphogenetic window, leading to a substantial increase in leaf complexity and leaflet number (Fig 2E) [48,51]. *crel-1 clau* double mutants had very complex leaves (Fig 2E and 2F), suggesting that CREL acts in parallel with CLAU to restrict leaf elaboration and promote maturation. Removing the activities of both regulators leads to prolonged, extensive leaflet morphogenesis. Together, these results suggest that CREL acts in relatively late stages of leaf development to promote maturation and differentiation.

The suppression of the *e* phenotype by *crel* raised the question of whether CREL is also involved in the differential growth at the leaf margin that leads to the formation of separate leaflets. To address this question, we crossed *crel* to mutants affected in auxin-mediated blade growth. Ectopic expression of a stabilized form of E resulting from a mutation in domain II of the E (IAA9) protein (EdII) resulted in leaflet narrowing [42], (Fig 2G). This effect was strongly enhanced in the *crel-1* background (Fig 2H), suggesting that E inhibits and CREL promotes blade expansion, but they act in at least partially parallel pathways. Similarly, *crel-1* enhanced the narrow blade phenotype resulting from ectopic expression of a miR160-resistant ARF10, a negative regulator of blade expansion (*FIL>>ARF10m*, Fig 2I and 2J). In agreement, *crel-1* suppressed the ectopic blade growth resulting from ectopic expression of miR160, which negatively regulates ARF10 and 4 additional ARF proteins (*FIL>>miR160*, Fig 2K and 2L) [40]. The suppression of *FIL>>miR160* was more prominent in later leaves than in early leaves (S2 Fig). Interestingly, leaflet number was reduced in *FIL>>ARF10 crel-1* relative to both single mutants, and *crel-1 FIL>>EdII-GUS* plants were extremely small with almost no leaflets, suggesting that extreme repression of lamina growth leads to a reduction in leaflet formation and overall growth. Together, these results suggest that CREL promotes blade growth during compound-leaf development, and acts at least partially in parallel to auxin.

CREL is a VRN5 homolog

To identify the *CREL* gene, we genetically mapped the *crel-1* mutation using an F2 mapping population from a cross between the *crel-1* mutant, in the *Solanum lycopersicum* M82 background, and *S. pimpinellifolium*. *crel-1* was mapped to chromosome 5. Further mapping was hampered by an introgression of *S. pimpinellifolium* sequences in the M82 line in this region [53]. We therefore used RNA-seq to identify possible causative mutations in *crel-1* and *crel-2*, which led to the identification of mutations in the gene *Solyc05g018390* in both *crel-1* and *crel-2*. In *crel-1*, a G to A substitution at position 4264 from the transcription start site (TSS) led to a stop codon in exon III. The fast neutron allele *crel-2* contains a 12,826-bp-long deletion, which results in the elimination of exon I and II and part of exon III (Fig 3A). Sequencing the Solyc05g018390 gene in two additional *crel* alleles identified a 1-bp deletion in the first exon at position 322 from the TSS in *crel-3*, and an A to T substitution in position 3630 leading to a stop codon in the third exon in *crel-5* (Fig 3A). We therefore concluded that Solyc05g018390 is *CREL*. *CREL* is predicted to encode a plant homeodomain (PHD) finger protein (Fig 3A and 3B). It is most similar to the Arabidopsis VRN5 gene.

CREL is expressed in expanding blades

We characterized the expression of *CREL* in the fifth leaf produced by the plant, at different developmental stages, to examine how its expression correlates with its activity. *CREL* was expressed throughout leaf development, with relatively low expression in apices containing the SAM and very young P1-P3 primordia. Later, its expression was gradually upregulated, peaking at P6/P7 (Fig 3C). To spatially localize *CREL* in leaf primordia, we cloned a 2960-long *CREL* promoter and used it to generate a CREL driver line in the transactivation system [52,56]. In developing leaves, the *CREL* promoter drove expression in leaf margins. In agreement with the qPCR experiment, expression appeared lower in young primordia, and increased from P4 on. Expression was mainly visible in expanding regions of the leaf margin, the terminal leaflet at P4, and the expanding leaflets at P6 and on (Fig 3D–3G). The expression appeared to follow the basipetal differentiation wave of the leaf, with strong expression first appearing in the terminal leaflet, which is the first to expand and differentiate, and then progressing basipetally in expanding leaflets. This leaf expression pattern is compatible with the

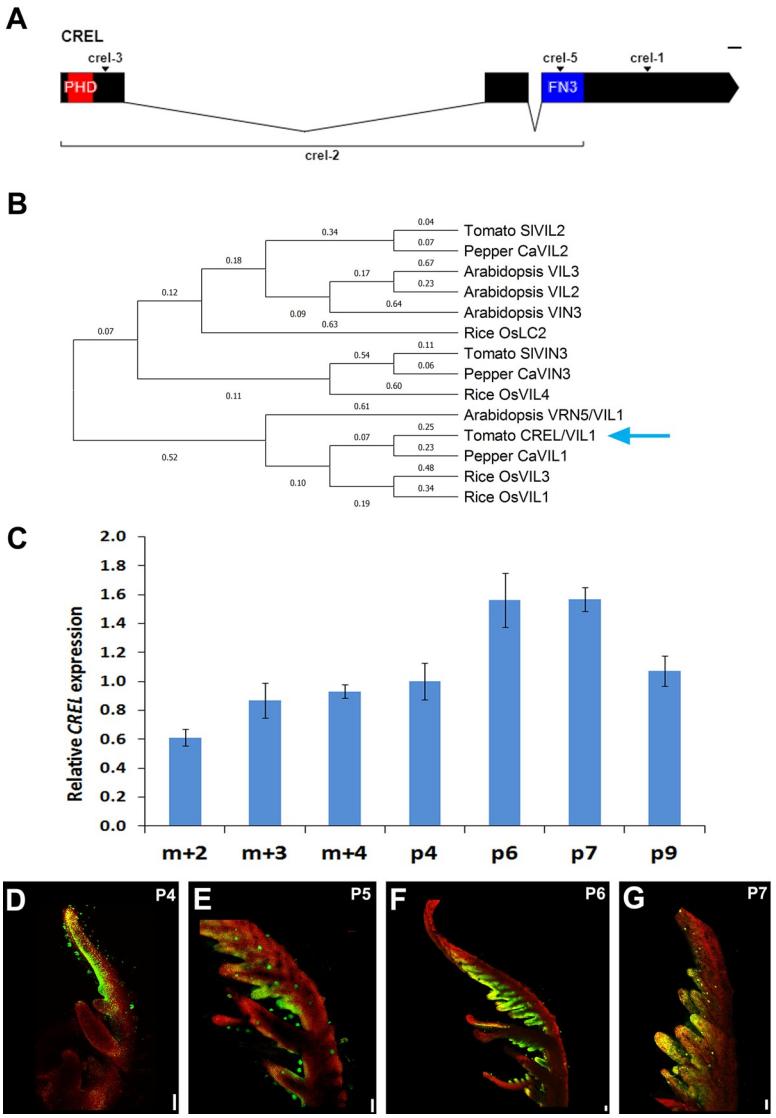

Fig 3. CREL encodes a VRN5/VIL1 homolog expressed at late stages of leaf development. (A) A diagram of the CREL (Solyc05g018390) gene. The boxes indicate exons and the combining lines introns. The location of the mutation in 4 *crel* alleles is indicated. (B) A phylogenetic tree of the tomato, Arabidopsis, rice and pepper VIL proteins, constructed using MEGA X [54,55] using a Maximum Likelihood method. Branch lenghts represent the expected number of substitutions per site. The blue arrow points to CREL. (C) qRT-PCR analysis of *CREL* mRNA expression at successive developmental stages of the 5th leaf. m+2, 3, or 4 represents the meristem and the 2, 3, or 4 youngest leaf primordia, respectively. P4-P9 represent isolated leaf primordia at the respective developmental stage (see Fig 1). Error bars represent the SE of at least three biological replicates. (D-G) Confocal images of leaf primordia of the indicated stages, expressing *pCREL>>YFP*, using the transactivation system, as in Fig 2. P4-P7 represent the 4^{th}-7^{th} youngest leaf primordia, respectively. In G, a leaflet from a P7 primordium is shown. Scale bars: 0.1 mm.

https://doi.org/10.1371/journal.pgen.1009633.g003

crel leaf phenotype, which starts to differ from the wild type around the P5 stage (Fig 1I), and with the genetic interactions showing that *crel* affects leaf maturation and blade formation (Fig 2).

CREL promotes multiple aspects of plant maturation and differentiation

In addition to their effect on leaf differentiation and patterning, additional differentiation processes were also delayed and/or impaired in *crel* mutants. *crel* plants failed to maintain an

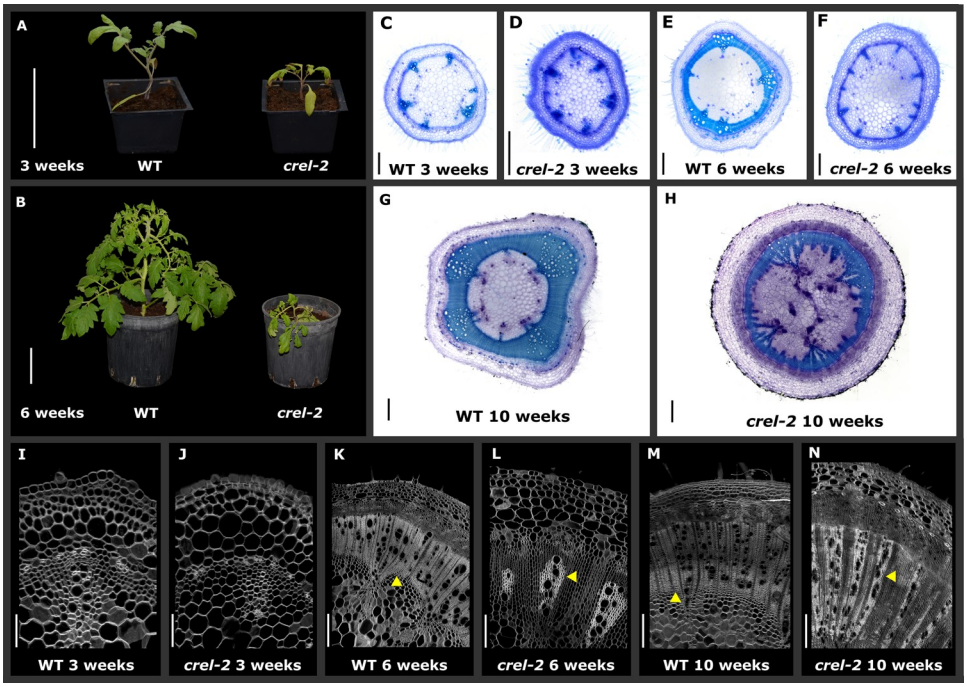

Fig 4. CREL promotes stem vasculature maturation and differentiation. (A, B) Whole plants of the indicated genotypes and ages. Scale bars: 10 cm. (C-H) stem cross sections, dissected from the first internode of the plant (between the hypocotyl and first leaves) at the indicated times after germination and stained with Toluidine blue. Scale bars: 500 mm. (I-N) Confocal images of stem cross sections, taken from the first internode of the plant at the indicated times after germination. Yellow arrowheads point to differentiated (WT) or undifferentiated (*crel-2*) xylem/vasculature. Scale bars: 100 mm (I,J); 200 mm (L); 500 mm (K,M,N).

https://doi.org/10.1371/journal.pgen.1009633.g004

upright position and the plants exhibited a sprawling growth habit. Similar to the effect on leaf shape, this phenotype developed at a relatively late stage of plant development (Fig 4A and 4B). To understand the basis for the "crawling" phenotype, we dissected developing wild-type and *crel-2* stems at successive developmental stages. We sectioned the internode between the cotyledons and the first leaf from different plants grown together, between the ages of 3 and 10 weeks. In three-week-old plants, *crel-2* stems were narrower than the wild type with nearly normal although slightly less developed vascular bundles (Fig 4C, 4D, 4I and 4J). *crel-2* vasculature continued to develop slower than the wild type, and ceased maturation and differentiation prematurely. This resulted in a thin and undeveloped xylem in *crel-2* stems. Specifically, *crel-2* stems failed to complete a vascular cylinder, and had only partial secondary xylem development (Fig 4E–4H, 4K–4N). The reduction in supporting tissue likely contributes to the reduced strength of the *crel* stem.

Root vasculature development was also delayed and impaired in *crel* mutants. *crel-2* roots were narrower than wild-type roots, and their vascular tissue developed slowly and failed to reach full differentiation (Fig 5A–5F). To investigate the effect of *crel* on the root system as a whole, wild type and *crel-2* plants were grown hydroponically, and root volume and length were calculated at successive times. Root volume and length were reduced in *crel-2* plants, and the difference increased with time, although the difference was statistically significant at one of the time points only (Fig 5G and 5H). Therefore, CREL plays an important role in root development and differentiation.

The *crel* mutation also affected flowering time and flower development. *crel-1* and *crel-2* mutants flowered much later than the wild type, after producing 12–13 leaves, compared to 6

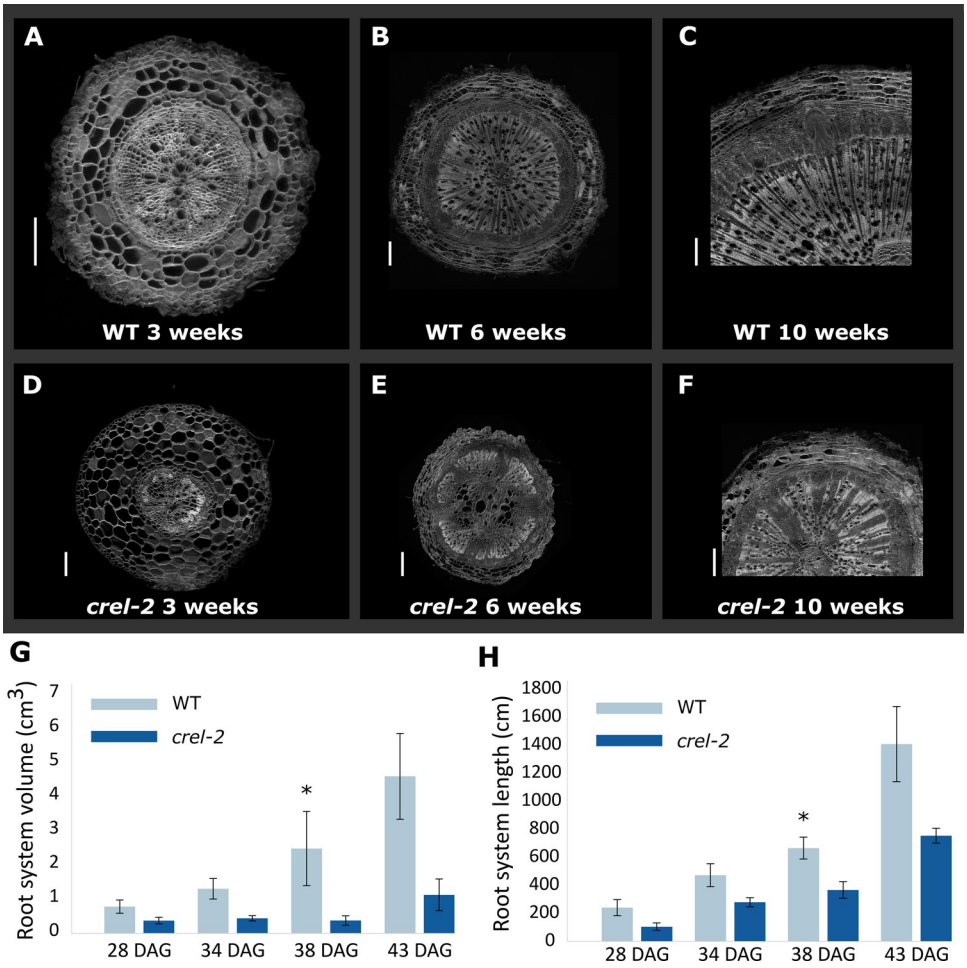

Fig 5. CREL promotes root development and differentiation. (A-F) Confocal images of root cross sections of the indicated genotypes dissected from the upper part of the primary root. Scale bars: 200μm (A, B, G); 500μm (C-F). (G) Root system volume at different times after germination, calculated with WinRhizo software. Shown are averages and SE of 3 plants (n = 3). Asterisks indicate statistically significant differences between *crel-2* and WT, by Student's t test, $^{*}p < 0.05$. (H) Root system length at different times after germination (DAG), calculated withWinRhizo software. Shown are averages and SE of 3 plants (n = 3). Asterisks indicate statistically significant differences between *crel-2* and WT, by Student's t test, $^{*}p < 0.05$.

https://doi.org/10.1371/journal.pgen.1009633.g005

leaves in the wild type (Fig 6A). Mature *crel* flowers were not fully developed, had short and distorted organs and were sterile (Fig 6B and 6C). Early flower development was similar between wild type and *crel* plants, except for the sepals that were curled backwards in *crel*, resulting in an open bud where the inner organs were not covered by the sepals. However, *crel* flower organs ceased development and growth prematurely (Fig 6D–6G). Therefore, *crel* mutants were delayed in multiple developmental pathways. In some cases such as flower, stem, and root development, these organs failed to properly differentiate, while in others, such as leaf development and flowering time, they differentiated substantially slower than the wild type. Overall, *crel* plants had aberrant plant and organ structure, which resulted in weak and sterile plants.

In Arabidopsis, VIL proteins affect flowering time by silencing the expression of the flowering repressor FLC. Three tomato genes were included in the FLC/MAF clade in a phylogenetic analysis of tomato MADS-box genes, *SlMBP8* (Solyc12g087830), *SlMBP15* (Solyc12g087820)

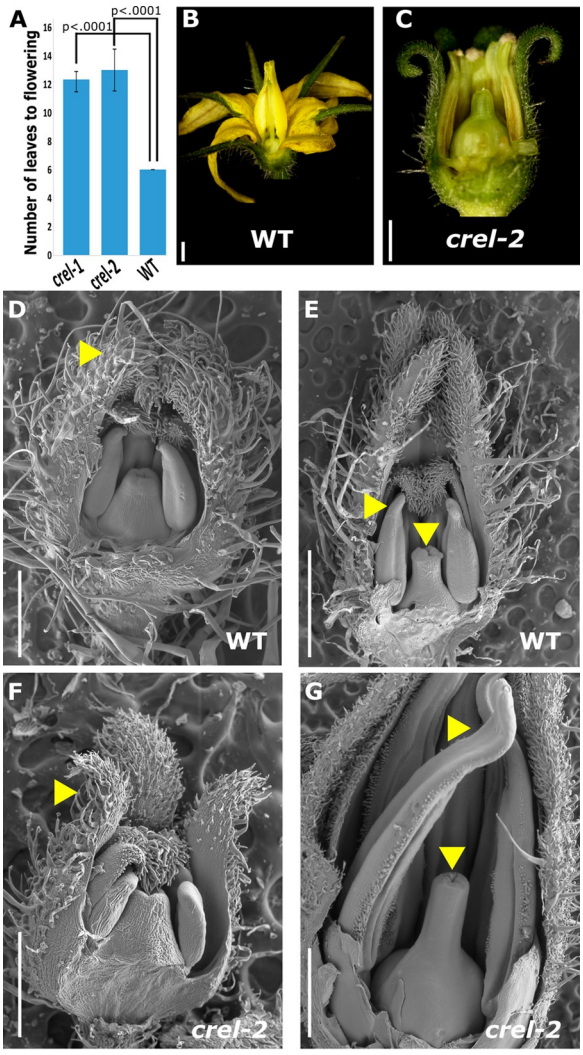

Fig 6. CREL promotes flowering, floral organ growth, and differentiation. (A) Flowering time, measured by number of leaves produced before flowering, of the indicated genotypes. Error bars represent the SE; *p*-values indicate differences from WT, as determined by Dunnett's test. n = 12 (wt, *crel-1*) and 4 (*crel-2*). (B, C) Stereoscope images of mature flowers. Scale bars: 1mm. (D-G) Scanning electron microscope (SEM) micrographs of the indicated genotypes at 2 early developmental stages. D, F—0.5 mm long stage 6 flowers; E, G—1 mm long stage 11 flowers (according to [57]. Yellow arrowheads point to normal (WT, D) and distorted (*crel-2*, F) young petals, and to normal (WT, E) and distorted (*crel-2*, F) stamens and stigma. Scale bars: 1mm (E, G); 0.5mm (D, F).

https://doi.org/10.1371/journal.pgen.1009633.g006

and *SlMBP25* (Solyc05g015730) [58] (S3A Fig). Of these, only *SlMBP8* shared a similar gene structure with *FLC*. *SlMBP8* showed reduced H3K27me3 enrichment in *crel-2* mutants and was upregulated about 2-fold in *crel-2* by qRT PCR (S3B–S3E Fig). Therefore, *SlMBP8* may be involved in the late flowering phenotype of *crel*, but further analysis is required to assess its role.

CREL mediates H3K27me3 modifications at a subset of polycomb-silenced genes

Homology of *CREL* to the Arabidopsis *VRN5* gene suggested that it may be involved in the repression of gene expression by promoting PRC2-mediated H3K27me3 modification. To test

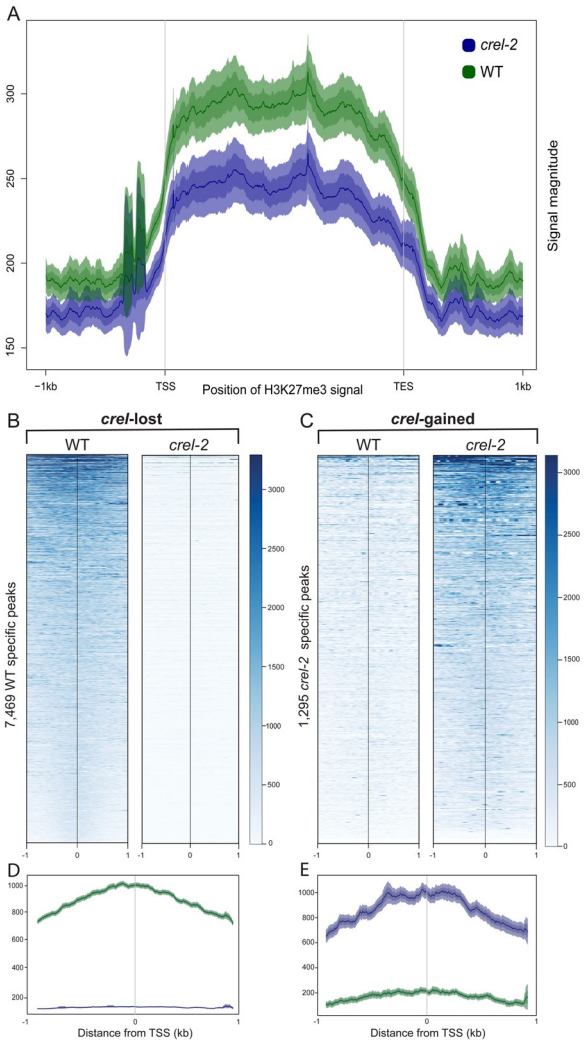

Fig 7. CREL mediates H3K27me3 modifications at a subset of polycomb-target sites. (A) Normalized H3K27me3 signal displayed across all protein-coding genes in WT and *crel-2* mutant shoot apices. (B) Heatmaps of H3K27me3 signals at 7,469 sites identified as reproducibly enriched in WT but lost in *crel-2* (*crel*-lost sites). Signals are centered in the middle of each enriched region and extend +/- 1 kb in each direction. (C) Heatmaps of H3K27me3 signals at 1,295 sites identified as reprodicbly enriched in *crel-2* plants but not in WT (*crel*-gained sites), displayed as in (B). (D) Average plots of WT and *crel-2* H3K27me3 at the 7,469 *crel*-lost sites shown in panel B. (E) Average plots of WT and *crel-2* H3K27me3 at the 1,295 *crel*-gained sites shown in panel C.

https://doi.org/10.1371/journal.pgen.1009633.g007

this prediction, we performed ChIP-seq for the H3K27me3 modification in shoot apices of 4-week-old wild-type and *crel-2* plants (S2 Table). In wild-type tissue, H3K27me3 was found to be enriched in a characteristic pattern over gene bodies, with *crel-2* mutants showing a decrease in average H3K27me3 over genes (Fig 7A). To determine whether this decrease was due to a small loss at all H3K27me3 sites or a large loss at a smaller number of sites, we identified all enriched sites found in two replicates for each genotype and compared these reproducibly enriched sites between wild-type and *crel-2*. Of the 14,789 reproducibly enriched regions in WT, 7,469 of these sites were essentially depleted of H3K27me3 in *crel-2* mutant plants (Fig 7B and 7D; *crel*-lost H3K27me3 sites). Interestingly, 1,295 sites showed increases in H3K27me3 in the *crel-2* mutant (Fig 7C and 7E; *crel*-gained H3K27me3 sites). The vast majority of these sites are normally enriched for H3K27me3 in wild-type, suggesting that in the

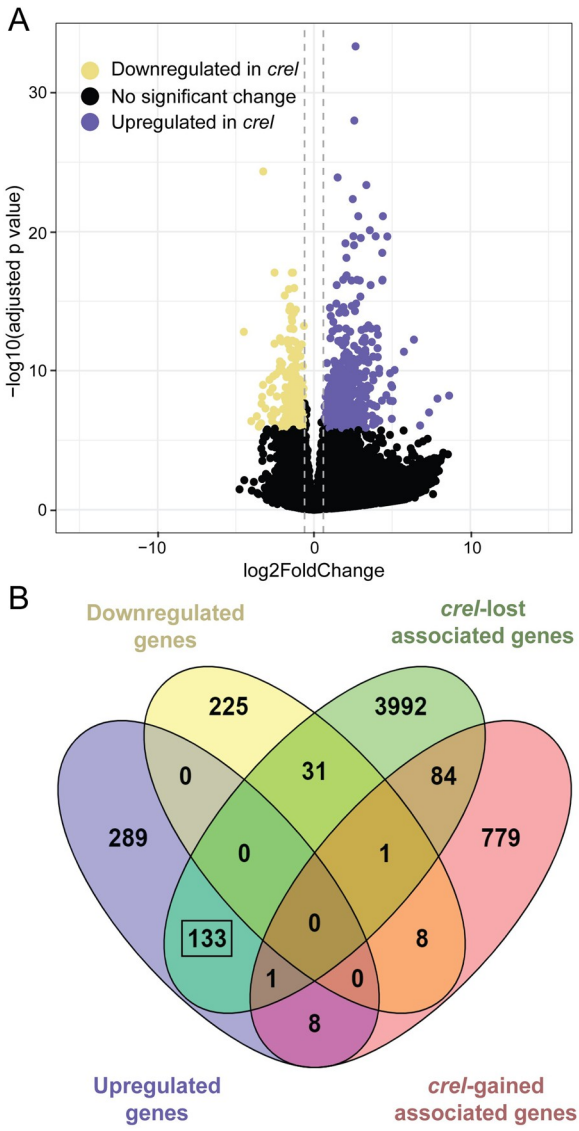

Fig 8. Changes in H3K27me3 deposition in *crel* mutant plants correlate to gene expression changes as measured by RNA-Seq. (A) Differential gene expression analysis of WT and *crel* shoot apices by RNA-seq. These data are illustrated in a volcano plot, with purple dots representing upregulated transcripts (adjusted p value < Bonferroni corrected significance threshold of 1.4e-6 and log2 fold change > 0.6) and yellow dots representing downregulated transcripts (adjusted p value < 1.4e-6 and log2 fold change < -0.6). Vertical dashed lines delineate log2 fold change thresholds of -0.6 and +0.6. Four hundred and thirty one (431) transcripts were significantly upregulated and 265 were significantly downregulated in *crel* plants compared to WT. (B) Venn diagram comparing the overlap of upregulated transcripts (purple) and downregulated transcripts (yellow) to genes associated with H3K27me3 peaks unique to WT (*crel*-lost sites; green) and unique to *crel-2* (*crel*-gained sites; green). The black box highlights overlap between upregulated transcripts and genes associated with WT unique peaks (*crel*-lost sites).

https://doi.org/10.1371/journal.pgen.1009633.g008

absence of CREL, excess PRC2 activity is directed to these sites that were only modestly enriched with H3K27me3 in wild-type. The *crel*-lost and *crel*-gained H3K27me3 site coordinates as well as associated genes are described in S3 Table.

To examine the effects of H3K27me3 loss on the transcriptome, we performed RNA-seq in multiple replicates on shoot apices of 4-week-old wild-type plants and plants with 3 independent *crel* alleles (Fig 8). RNA was prepared from a total of seven biological replicates of *crel* mutant

plants and compared to three biological replicates of wild-type *S. lycopersicum*. Differential gene expression analysis revealed that 431 genes were significantly upregulated in all *crel* mutants and 265 were significantly downregulated compared to the wild-type (Fig 8A and S4 Table). Gene ontology analysis utilizing agriGO [59] showed significant enrichment among these upregulated genes for the biological function "Transcription Factor Activity" (FDR = 8.1e-6) and other terms associated with transcriptional regulation (S5 Table). The genes downregulated in *crel* mutants showed no significantly enriched GO terms using the same parameters.

To understand the relationship between chromatin alterations and transcriptional changes in *crel*, we mapped the *crel*-lost and *crel*-gained H3K27me3 sites to genes. The 7,469 *crel*-lost sites were associated with 4,242 genes, 133 of which were also upregulated in *crel* mutants (of 431 total upregulated genes) (Fig 8B and S6 Table). This reinforces that loss of CREL results in changes in gene expression by affecting H3K27me3 deposition at a subset of genes. While not all genes associated with *crel*-lost H3K27me3 peaks showed significant gene expression changes under the stringent expression criteria used, when statistical significance is not considered the majority of the genes that lose H3K27me3 in *crel* have log2 fold changes greater than 0 (S5 Fig). As many aspects of plant and organ maturation and differentiation are delayed and/or impaired in *crel* mutants, we asked whether the molecular signature of maturation and differentiation is affected in *crel*. Israeli et al. (2021) [32] defined sets of "morphogenesis" and "differentiation" genes based on transcriptomic data of successive stages of leaf development as well as mutants that affect morphogenesis and differentiation. We examined whether there is an enrichement in "differentiation" and "morphogenesis" signatures among genes that showed altered expression and/or altered H3K27me3 modifications in *crel*. This analysis showed that "differentiation" genes were significantly enriched among the genes that were downregulated in *crel*, with 4 times more "differentiation" genes then expected by random overlaps between groups being present in the subset of genes that were significantly down-regulated in *crel* (p-val $<$ 8.509e-15, S7 Table).

Discussion

VIL proteins have been shown to affect flowering in several plant species, by repressing the expression of flowering repressors, such as *FLC* in Arabidopsis. In addition to their effect on flowering, VIL genes were found to affect an array of developmental processes in different species. This work identifies the tomato VIL gene *CREL* as a mediator of diverse developmental processes, via the modulation of H3K27me3 modifications in many genes throughout the tomato genome, likely by recruiting PRC2 complexes to a subset of their target genes.

CREL promotes plant and organ maturation

So far, VIL genes have been mainly implicated in flowering time [7,14,16,18,20–22,25,60]. Here, we uncover a much broader role for this gene family in plant development, as revealed from the phenotypes and the effect on H3K27me3 modification. *crel* mutants are affected in many aspects of plant maturation and differentiation in addition to the delay in flowering time. *crel* mutants flower late and have delayed leaf maturation, resulting in an extended leaf morphogenesis and more compound leaves. Interestingly, while flowering and leaf maturation eventually occur in *crel*, stem, root, and flower differentiation are impaired in *crel* and these organs do not reach full differentiation and function. CREL accumulates relatively late during leaf development, thus enabling prolonged morphogenesis. Recently, a growth-rate dependent mechanism of controlling VIN3 accumulation in the cold has been described [61]. It would be interesting to understand the mechanism by which CREL expression is delayed during organ maturation to enable timed maturation and differentiation.

Other genes involved in the induction of flowering were also shown to affect maturation and differentiation in additional developmental aspects. For example, the tomato flowering inducer SFT, the ortholog of FT, was shown to promote leaf maturation and affect stem differentiation [62]. Recently, SFT was shown to specifically affect secondary cell wall biosynthesis in tomato stems [63]. FT was also proposed to promote maturation and termination in additional species [64,65]. The pepper *cavil1* mutants, impaired in the pepper *CREL* ortholog, have reduced vascular development but wider stems [25]. Therefore, both precocious and delayed differentiation impairs the final form and function of stems. In *Cardamine hirsuta*, plant maturation and flowering was shown to be coordinated with age-dependent changes in leaf shape in plants with variable FLC activity [66]. In contrast to CREL and SFT, which promoted all aspects of plant and organ maturation, tomato CIN-TCPs were shown to promote leaf maturation but delay plant maturation, while AP1/FUL MADs BOX genes promoted plant maturation and delayed leaf maturation [67,68]. Overall, similar to *CREL*, genes that have been implicated mainly in the promotion of flowering in Arabidopsis were found to promote a wide range of differentiation and maturation aspects.

The involvement of CREL in plant and organ differentiation is in agreement with a role in mediating PRC2 activity. A common function of PRC2 genes in plants is the maintenance of a differentiated state, and *prc2* mutants in both mosses and seed plants have phenotypes related to dedifferentiation and overproliferation [1,2,69]. Therefore, CREL may aid in recruiting PRC2 to differentiation-related target genes.

VIL genes from other species have also been shown to affect other developmental processes in addition to flowering. [13,16,19,21,25,26]. Interestingly, beside the common effect on flowering time, the specific developmental effects only very partially overlap among these species. This suggests that the VIL family may be used as a tool for developmental innovations, recruiting an existing tool to different processes. Specifically interesting in this respect is the comparison between tomato and pepper, which are closely related species that differ in several key developmental features, such as flowering architecture and leaf shape. *cavil1* mutants have reduced vasculature development, increased plant and organ size, increased branching and reduced angle of axillary branches [25]. Interestingly, only some of these additional phenotypes overlap with *crel*. In contrast to the simple leaves of pepper, tomato leaves are compound, with several orders of leaflets. This is correlated with faster differentiation of the pepper leaf, similar to tomato *La-2/+* mutants [29]. The current work revealed an important role for CREL in the development of the compound leaf, with an effect on both the rate of differentiation and leaf patterning (Figs 1 and 2), further supporting the notion that VIL genes have been recruited to diverse, partially species-specific processes.

We propose that, in addition to its general effect on growth and differentiation, CREL also promotes blade growth in developing tomato leaves. *crel* mutants suppress the ectopic blade outgrowth of *e* mutants and miR160-overexpressing plants (Figs 2K and 2L, S2). Furthermore, *crel* enhances the narrow-leaf phenotype caused by overexpression of *E* or miR160-targeted ARFs. In addition, *CREL* expression is elevated in later stages of leaf development when the blade begins to expand, and the *CREL* promoter shows high expression in growing regions of the leaf margin (Fig 3D–3G). The genetic interactions between *crel* and auxin-related mutants suggest these auxin mediators and CREL act via independent pathways to regulate blade growth. Therefore, CREL likely promotes blade growth either downstream of auxin or through an at least partially parallel pathway. As most effectors of compound-leaf development have been shown to affect either the organ-level differentiation rate (for example LA and CLAU) or local differential growth (E, CUC, SlMP) [27], it is interesting that CREL appears to affect both aspects.

CREL affects H3K27me3 modifications throughout the tomato genome

Only a handful of VIL targets have been identified so far, most of which are related to their role in promoting flowering. In Arabidopsis, FLC and FLC-related proteins are targeted by different VIL proteins in specific flowering pathways [11,14]. In rice, the flowering inhibitors *OsLF* and *OsLFL1* were identified as VIL targets [18,22,70]. In addition, a cytokinin catabolism gene from the CKX family and the bud-outgrowth inhibitor OsTB1 have been identified as a VIL target in rice [19,26]. The microRNA miR156 was proposed as a target of BdVIL*4* in *Brachypodium* [21], and several putative targets have been proposed to mediate the effect on flowering of pepper VIL1 [25]. Here we found that of the 14,789 sites enriched with H3K27me3 in wild-type plants, approximately half (7,469) lose nearly all H3K27me3 in *crel* mutants. The identification of such a global effect on H3K27me3 modification in *crel* mutants indicates that this VIL protein has a widespread role in polycomb silencing. Together with the pleiotropic phenotypic effect, this suggests that VIL proteins are involved in a wide range of developmental processes, and play a central role in recruiting PRC2 complexes to many targets genome wide. The similarly pleiotropic effect of *Cavil1* mutants in pepper, together with its effect on gene expression [25], suggests that this is also true in other species.

Interestingly, the widepsread reductions in H3K27me3 across the genome in *crel* are also associated with gains in H3K27me3 at a smaller number of sites (1,295) that normally have modest levels of the H3K27me3 mark in wild-type plants. This phenomenon of H3K27me3 redistribution in PRC2-targeting mutants has been previously observed in both plants and animals [8,71] and suggests that sufficient PRC2 activity is a limiting factor in H3K27me3 accumulation under normal circumstances. However, we are aware that, prior to mapping the CREL binding sites, we cannot rule out that CREL plays a role in targeting PRC2 activity to many loci while directly inhibiting it at others. This distinction awaits future experimental testing.

A conserved role for VIL genes in promoting flowering

VIL genes have been shown to affect flowering time in many species where mutations or silencing of these genes have been described, including both dicots and monocots [7,14,16,18,20,22,25]. In Arabidopsis, VIL proteins promote flowering by recruiting PRC2 to flowering repressors from the FLC family, thus facilitating the deposition of the repressive chromatin modification H3K27me3. Different Arabidopsis VILs act to induce flowering in specific combinations of flowering pathways, timing and target genes [11,14]. Interestingly, while tomato plants do not require vernalization for flowering, *crel* mutants are late flowering. Similarly, VIL genes promote flowering in additional species that do not require vernalization for flowering, or in species with a different vernalization mechanism. Rice VIL proteins including LC2 were shown to act by repressing *OSLFL1* and *OsLF*, two flowering repressors unrelated to FLC [18,22,70]. Therefore, while the effect on flowering and possibly the molecular mechanism are conserved, the target genes differ among species [25]. While the FLC homolog *SlMBP8* (Solyc12g087830.1) shows reduced H3K27me3 enrichment in *crel-2* (S3 Fig), further research is required to understand whether it mediates the *crel* late-flowering phenotype.

Materials and methods

Plant material and growth conditions

Tomato plants (*Solanum lycopersicum* cv M82) were germinated and grown in a controlled growth room or in a commercial nursery for four weeks. Then the seedlings were transferred to a greenhouse with natural daylight and 25˚C/ 20˚C day/night temperature, or to an open field with natural daylight and temperature. *crel-1* was isolated in this work by a mutant screen in the *e-3* background (Berger 2009, Ben Gera 2012), as described below. *crel-2—crel-5* are

from the mutant populations described by Menda et al.,[44]. The transactivation system, described previously [52,56], was used to characterize the CREL promoter and for leaf-specific expression. This system consists of driver lines and responder lines. In the driver lines, specific promoters drive the expression of the synthetic transcription factor LhG4, which does not recognize endogenous plant promoters. In the responder lines, a gene of interest or a reporter is expressed downstream of the E.coli operator, recognized by LhG4 but not endogenous plant transcription factors. A cross between a driver and a responder line results in a plant (designated PROMOTER>>GENE) expressing the gene of interest/marker under the control of the specific promoter. *La-2*, *clau*, the *FIL* driver line and the *ARF10*, *miR160* and *EdII-GUS* responder lines have been previously described [35,40,47,51,52,72].

Generation of a mutant population, screening and identification of *crel-1*

Around 750 *entire-4* (*e-4*) seeds were treated with the mutagenic substance Ethyl-Methane Sulfonate (EMS, Sigma m0880) at a concentration of 0.6% for 10 hours. Around 50 seeds underwent a control treatment without exposure to EMS. The treated seeds were sown in a commercial nursery and the seedlings (M1 generation) were transferred to a greenhouse. M1 plants were self-pollinated to increase the number of seeds per plant. M2 seeds were collected separately from each of around 650 M1 plants. M2 progeny (around 40 seeds per family) were grown in an open field, and screened frequently during the season for mutants that affect the development of the leaf, flower and fruit. *e crel-1* was identified in this screen as a recessive mutant segregating 1:3 in an M1 family. Single *crel-1* mutants were generated by a cross between *e crel-1* and wild type and identification of single *crel-1* mutants in the F2 generation. *crel-1* was then back-crossed three times to M82 for further characterization.

Allelism tests and genetic interactions

As *crel* mutants are sterile, allelism tests were performed by crossing heterozygote siblings. Progeny of a cross between two heterozygous alleles segregated ¼ mutant progeny. Similarly, genetic interactions between *crel* and other mutants or transgenic lines were generated by crossing heterozygous *crel* siblings with the respective mutant or transgenic line.

Identification of the *CREL* gene

An F2 mapping population was generated by crossing *crel-1*/+ plant, in the M82 background to *Solanum pimplinellifolium*, and collection of F2 progeny from individual F1 plants. Initial mapping with 30 F2 plants showing the *crel-1* phenotype, and 50 mapping markers developed by Revital Bronstein, Yuval Eshed (Weizmann Institute) and Zach Lippman (CSHL) and spread along the tomato genome, identified linkage to 3 markers on chromosome 5. Fine mapping of 120 *crel-1* F2 individuals and additional markers located the gene to a region between markers zach 43.2 and jose 58.1 dcap, located between bases 43,123,344 and 58,170,500 on chromosome 5. Further mapping was hampered by an introgression of *S*. *pimpinellifolium* sequences in the M82 line in this region [53] We therefore used RNAseq of wild type, *crel-1* and *crel-2* plants to identify polymorphism in these alleles.

For RNAseq, shoot apices containing the SAM and the 4 youngest primordia were collected from 14-day-old M82, *crel-1* and *crel-2* plants, in which L4 (the 4th leaf produced by the plant) was at the P4 stage. RNA was extracted using the RNeasy micro kit (Qiagen), using the manufacturer's instructions. Two biological replicates were used for M82 and *crel-2*, and one biological replicate for *crel-1*. Sequencing libraries were prepared according to the Illumina TruSeq RNA protocol and sequenced on an Illumina HiSeq2000 platform at the Genome Center of the Max Planck Institute for Plant Breeding Research. We obtained between 21,3 and 28,3

million 96-bp single-end reads per library (average of 25,8 million). Reads were aligned to the *S. lycopersicum* reference sequence v2.40 using TopHat v2.0.6 [73] with the following parameters: -max-insertion-length 12 -max-deletion-length 12 -g 1 -read-gap-length 12 -read-edit-dist 20 -read-mismatches 12 -no-coverage-search -read-realign-edit-dist 0 -segment-mismatches 3 -splice-mismatches 1. To detect polymorphisms between the *crel* mutants and wild-type M82, biological replicates from each genotype were merged. Then, duplicated reads were removed using default settings in Picard (http://broadinstitute.github.io/picard/), indels were realigned using GATK v2.2–8, and variants called in all samples simultaneously using default parameters in GATK v2.2–8 [74]. Next, we estimated the effect of each variant in annotated transcripts (ITAG 2.3) using ANNOVAR [75]. Variants in the candidate region in chromosome 5 determined by QTL analysis were evaluated manually.

Phenotyping and imaging

Characterization of early leaf development and rate of leaf initiation. Plants were sown, germinated and grown in a growth chamber. Every two weeks, the number of leaves and leaf primordia were counted from six plants from each genotype. The fifth leaf (L5) was photographed by a stereoscope (Nikon SMZ1270) and its developmental stage determined. Six different plants were used for each time point.

Quantification of leaf complexity. Leaves 5, 7 and 9 were marked at the time of their emergence from the shoot apex. Then, the number of leaflets was counted every 7–14 days for each marked leaf. Primary, intercalary, secondary and tertiary leaflets were counted. At least 9 plants were counted for each genotype.

SEM characterization of flower development. Flowers from different developmental stages of each genotype were collected and their petals removed using a stereoscope, placed on a microscope stub with a carbon strip and analyzed with Hitachi TM3030 Plus SEM.

Phenotypic quantification and statistical analysis. For the quantification of the number of leaves to flowering, plants were grown in a greenhouse, and with the appearance of the first flower, the number of leaves formed before the flower were counted. At least 9 biological repeats, each consisting of a single plant, were quantified. The experiment was repeated twice, once with plants germinated in a commercial nursery and once with plants germinated in a growth chamber. For the quantification of root phenotypes, seedlings were grown hydroponically in Hoagland nutrient solution (pH 6.5), in a growth room set to a photoperiod of 12/12-h night/days, light intensity (cool-white bulbs) of $\sim$250 μmol m^{-2} s^{-1}, and 25˚C. After 28, 34, 38 and 43 DAG the roots of 3 plants of each genotype were scanned and analyzed using a flatbed scanner (Epson 12000XL, Seiko Epson, Japan) and root architecture was analysed using WinRhizo software (Regent Instruments Ltd., Ontario,Canada). Statistical analysis was performed using the JMP software (SAS Institute, http://www.sas.com). Means and p values were calculated using the Student's t-test or the Dunnett's test, as indicated in the figures.

Histological characterization of stem tissues. Ten to 50 day-old plants were free-hand dissected using a double-sided razor blade. 1-2-mm-long sections were dissected from up to 5 cm below the node. Sections were dehydrated in acetic acid: ethanol [1:10] for 1 hour and then stained directly with TBO (0.01% aqueous, sigma). Images of early developmental stages were captured using Nikon a SMZ1270 stereoscope equipped with a Nikon DS-Ri2 camera and NIS-ELEMENTS software.

Confocal imaging. For analysis of pCREL:nYFP expression, dissected whole-leaf primordia were placed into drops of water on glass microscope slides and covered with cover slips. The pattern of YFP expression was detected by a confocal laser scanning microscope (CLSMmodel SP8; Leica), with the solid-state laser set at 514 nm for excitation and 530 nm for emission. Chlorophyll expression was detected at 488nm for excitation and 700nm for

emission. ImageJ software was used for analysis, quantification, and measurements of captured images. Images were adjusted uniformly using Adobe Photoshop CS6. Tomato stems and primary roots were cut to sections of 200um and 300um width respectively using Leica VT1000 vibratome and were and cleared using ClearSee [76], cell wall staining was performed using SR2200 (Renaissance Chemicals) prior to mounting and visualization using 405nm laser.

Cloning and plant transformation

The *CREL* promoter was generated by amplifying 3000 bp upstream of the *CREL* ATG from genomic DNA and cloned upstream to LhG4 generating the *pCREL*:*LhG4* driver line.

Plant transformation and tissue culture were performed as described in Israeli et al 2019 [39]. At least five independent kanamycin-resistant transgenic lines from each transgene were genotyped and, in the case of *pCREL*:*LhG4*, crossed to an *OP*:*YFP* stable line to generate pCREL>>YFP. Three lines from each transgene or resultant cross were examined, and a representative line was selected for further analysis.

Phylogenetic analysis

Phylogenetic analysis was performed using full-length protein sequences of the tomato, Arabidopsis, rice and pepper VIL gene family or the FLC/MAF MADS-BOX clade. The sequences were obtained from the Sol Genomics Network (SOL, https://solgenomics.net/), The Arabidopsis Information Resource (TAIR, https://www.arabidopsis.org/) and the Plaza tool (https://bioinformatics.psb.ugent.be/plaza/). Sequences were aligned and phylogenetic trees were constructed using MEGA X [54,55], using using a Maximum Likelihood method, branch lengths represent the expected number of substitution per site.

RNA extraction and qRT-PCR analysis

RNA was extracted using the Plant/Fungi Total RNA Purification Kit (Norgen Biotek, Thorold, ON, Canada) according to the manufacturer's instructions, including DNase treatment. cDNA synthesis was performed using the Verso cDNA Kit (Thermo Scientific, Waltham, MA, USA) using 1 μg of RNA. qRT-PCR analysis was carried out using a Corbett Rotor-Gene 6000 real-time PCR machine, with SYBR Premix for all other genes. Levels of mRNA were calculated relative to *EXPRESSED* (*EXP*) [77] or *TUBULIN (TUB)* [78] as described [29]. Primers used for the qRT-PCR analysis are detailed in S1 Table.

ChIP-seq procedures

WT and *crel* plants were grown on soil under 16 hrs of light/8 hrs dark cycles for 28 days after germination. Shoot apices, (0.8 g for each replicate and two replicates per genotype) containing approximately three visible expanding leaves, were harvested and fixed in 1% formaldehyde + 0.2% Silwet L-77 for 17 minutes under vacuum. Glycine was then added to a final concentration of 0.125 M and tissue was placed under vacuum for an additional 5 minutes, followed by washing several times in water. ChIP was performed on the fixed tissue using the procedure of Gendrel et al. [79]. For each ChIP reaction, we used 2 ug of a rabbit polyclonal antibody against H3K27me3 (Millipore, catalog #07–449). Input and ChIP DNAs were converted to Illumina sequencing libraries using the Accel-NGS 2S Plus DNA library kit according to the manufacturer's instructions (Swift Biosciences). Libraries were sequenced on an Illumina NextSeq 500 instrument using 50-nt single end reads at the University of Georgia Genomics and Bioinformatics Facility.

ChIP-seq data processing

Raw reads were mapped to the SL3.0 build of the tomato genome using Bowtie2 [80] with default parameters. Raw mapped reads were then processed using Samtools [81] to retain only those with a mapping quality score greater than or equal to 2 and PCR duplicates were removed using Samtools "*rmdup*" function. Enriched regions (peaks) for H3K27me3 were then identified for each replicate using the "*Findpeaks*" function of the HOMER package [82]. Further analyses only considered peaks that were identified in both replicates for each genotype and reads were scaled to the lowest read depth using Samtools "*view -s*" function. Unique WT and *crel* sites were detected by using the Bedtools "*subtract*" function with the -wa parameter, where only peaks that were completely lost in either WT or *crel-2* were retained. These unique peaks from WT and *crel-2* were mapped to their nearest TSS using the "*annotatePeaks.pl*" function from the HOMER package [77]. See S2A Table for more information on read count numbers after each of these steps. For normalization and visualization, quality-filtered reads in.*bam* format were converted to *bigwig* format using the "*bamcoverage*" script in deepTools 2.0 [83] with a bin size of 1 bp and RPKM normalization. Heat maps and average plots displaying ChIP-seq data were also generated using SeqPlots visualization software [doi: 10.12688/wellcomeopenres.10004.1].

RNA-seq library preparation and sequencing

Wild-type and *crel* mutants shoot apices were grown and harvested as for ChIP-seq, and RNA was prepared using the Qiagen RNeasy Mini Plant kit according to the manufacturer's instructions. This included 3 biological replicates of wild-type tissue and 7 biological replicates from *crel* mutants (from 3 indpendent alleles: *crel-1*, *crel-2*, and *crel-3*). RNA-seq libraries were prepared using the Zymo RiboFree Total RNA Library Kit according to the manufacturer's instructions and libraries were sequenced using paired-end reads on an Illumina NovaSeq 6000.

RNA-seq data processing

Adapter sequences from raw RNA-Seq reads were trimmed using the "*ILLUMINACLIP*" function from the Trimmomatic software package using standard paired-end parameters. Trimmed reads were then mapped to the SL3.0 build of the tomato genome using the Spliced Transcripts Alignment to a Reference (STAR) aligner [84] with default parameters. Mapped reads were annotated to genes using the "*featureCounts*" function from the Subread software package. Differential gene expression analysis was calculated by using DeSeq2 package [85] comparing all *crel* mutant samples (3 independent alleles, 7 total biological replicates) together against wild-type data (3 biological replicates). See S4 Table for DeSeq2 output. For our analysis, only genes with adjusted p-values that met our Bonferroni-corrected p-value threshold of 1.395673e-06 (0.05/total # of genes detected; 35825) were considered. From there, differentially expressed genes were sorted into three bins: upregulated, downregulated, if log2 fold change from WT was over 0.6, less than -0.6 or from -0.59–0.59, respectively. See S2 Table for information on read processing numbers.

Enrichment analysis

The representation factor determines whether genes from one list (list A) are enriched in another list (list B), assuming that these genes behave independently. The representation factor is defined as: (number of genes in common between both lists)*(number of genes in the genome)/(number of genes in list A)*(number of genes in list B). p-values were calculated using exact hypergeometric probability [86].

Supporting information

S1 Fig. Characterization of *crel* mutants. (A-D) Mature 5th leaves of the indicated genotypes. White arrowheads point to primary and intercalary leaflets. Scale bars: 2cm. (E) Slower leaf production in *crel-2*. The Y axes shows the developmental stage (plastochron, P) of the fifth leaf produced by the plant at the indicated days after seeding. Error bars indicate SD (n = 5–11).
(TIF)

S2 Fig. Gradual suppression of FIL>>miR160 by *crel-1*. Mature 1st– 9th (L1-L9) of FIL<>miR160 (top) and crel-1 FIL>>miR160 (bottom). Scale bars: 2cm.
(TIF)

S3 Fig. A potential candidate for FLC in Tomato. (A) A phylogenetic tree of the Arabidopsis and tomato FLC-MADS BOX proteins, constructed using MEGA X [54,55] using a Maximum Likelihood method. For FLC, SlMBP8, SlMBP15 and SlMBP25 protein lengths and domains are illustrated. (B-D) qRT-PCR analysis comparing the mRNA expression of *SlMBP*8 (Solyc12g087830), *SlMBP15* (Solyc12g087820) and *SlMBP25* (Solyc05g015730) in whole shoots containing the SAM and 5 youngest leaf primordia from wild type (WT) and *crel-2* plants. *SlMBP8* mRNA expression levels were upregulated in *crel-2* compared to the WT. Error bars represent the SD of at least three biological replicates. (E) H3K27me3 enrichment -5434 upstream of the *SlMBP8* gene in wild type and *crel-2* shoot apices. C H3K27me3 was lost in *crel-2* in comparison to the wild type. Bars represent the average of 2 biological replicates, and error bars indicate SD.
(TIF)

S4 Fig. Overview of ChIP-seq datasets. Principal component analysis of input DNA and ChIP-seq samples.
(TIF)

S5 Fig. Overlap of genes mapped to ChIP-Seq peaks and RNA-Seq from *crel* mutants. This Venn Diagram shows the overlap between all transcripts detected by RNA-seq with log2 fold change equal to or less than 0 (yellow) and transcripts with log2 fold change over 0 (blue) compared to genes associated with H3K27me3 peaks unique to WT (*crel*-lost sites; green) and unique to *crel-2* (*crel*-gained sites; red).
(TIF)

S1 Table. Primers used in this work.
(DOCX)

S2 Table. Sequence read numbers for ChIP-seq. Two biological replicates of ChIP-seq for H3K27me3 were performed on shoot apices of WT and *crel1-2* plants. The table indicates for each biological replicate the number of total sequencing reads obtained, the number and percentage mapping to the tomato genome, and the total number of reads remaining after filtering for mapping quality. Reads with a MAPQ score of 2 or greater were used for further analysis.
(XLSX)

S3 Table. Genes associated with *crel*-gained and *crel*-lost H3K27me3 sites and the peak coordinates for these sites.
(XLSX)

S4 Table. Results output from DeSeq2 comparing all 7 *crel* replicates to the three WT replicates.
(XLSX)

S5 Table. Gene ontology analysis of all Upregulated genes in *crel* and all genes associated with *crel*-lost H3K27me3 sites.
(XLSX)

S6 Table. Overlap between: 1. *crel* upregulated genes and genes associated with crel-lost H3K27me3 sites; 2. *crel* downregulated genes and genes associated with *crel*-increased H3K27me3 sites.
(XLSX)

S7 Table. Anlaysis of enrichemnt of "differentiation" and "morphogenesis genes in the lists of *crel*-upregulated genes, *crel*-downregulated genes, genes associated with *crel*–increased H3K27me3 siets and genes associated with *crel*-lost H3K27me3 sites.
(XLSX)

Acknowledgments

We thank Yuval Eshed, Alon Samach and Dani Zamir for plant material and fruitful discussions and suggestions; Michael Lach for technical help, members of the Ori lab for continuous discussions and help; Revital Bronstein, Yuval Eshed and Zach Lippman for sharing the tomato mapping marker set.

Author Contributions

Conceptualization: Ido Shwartz, Neta Kovetz, Alon Israeli, Roger B. Deal, Naomi Ori.

Data curation: Katherine L. Duval, Ellen G. Krall, José M. Jiménez-Gómez, Roger B. Deal.

Formal analysis: Ido Shwartz, Chen Yahav, Matan Levy, Alon Israeli, Maya Bar, Katherine L. Duval, Ellen G. Krall, José M. Jiménez-Gómez.

Funding acquisition: Roger B. Deal, Naomi Ori.

Investigation: Ido Shwartz, Chen Yahav, Neta Kovetz, Matan Levy, Alon Israeli, Maya Bar, Katherine L. Duval, Ellen G. Krall, Naama Teboul, José M. Jiménez-Gómez, Roger B. Deal, Naomi Ori.

Supervision: Roger B. Deal, Naomi Ori.

Writing – original draft: Ido Shwartz, Chen Yahav, José M. Jiménez-Gómez, Roger B. Deal, Naomi Ori.

Writing – review & editing: Ido Shwartz, Chen Yahav, Neta Kovetz, Matan Levy, Alon Israeli, Maya Bar, Ellen G. Krall, Naama Teboul, José M. Jiménez-Gómez, Roger B. Deal, Naomi Ori.

References

1. Mosquna A, Katz A, Decker EL, Rensing SA, Reski R, Ohad N. Regulation of stem cell maintenance by the Polycomb protein FIE has been conserved during land plant evolution. Development. 2009; 136: 2433–2444. https://doi.org/10.1242/dev.035048 PMID: 19542356
2. Hennig L, Derkacheva M. Diversity of Polycomb group complexes in plants: same rules, different players? Trends Genet. 2009; 25: 414–423. https://doi.org/10.1016/j.tig.2009.07.002 PMID: 19716619
3. Xiao J, Wagner D. Polycomb repression in the regulation of growth and development in Arabidopsis. Curr Opin Plant Biol. 2015; 23: 15–24. https://doi.org/10.1016/j.pbi.2014.10.003 PMID: 25449722

4. Geisler SJ, Paro R. Trithorax and polycomb group-dependent regulation: A tale of opposing activities. Development. Company of Biologists Ltd; 2015. pp. 2876–2887. https://doi.org/10.1242/dev.120030 PMID: 26329598

5. Xiao J, Jin R, Yu X, Shen M, Wagner JD, Pai A, et al. Cis and trans determinants of epigenetic silencing by Polycomb repressive complex 2 in Arabidopsis. Nat Genet. 2017; 49: 1546–1552. https://doi.org/10.1038/ng.3937 PMID: 28825728

6. Zhou Y, Wang Y, Krause K, Yang T, Dongus JA, Zhang Y, et al. Telobox motifs recruit CLF/SWN-PRC2 for H3K27me3 deposition via TRB factors in Arabidopsis. Nat Genet. 2018; 50: 638–644. https://doi.org/10.1038/s41588-018-0109-9 PMID: 29700471

7. De Lucia F, Crevillen P, Jones AME, Greb T, Dean C. A PHD-Polycomb Repressive Complex 2 triggers the epigenetic silencing of FLC during vernalization. Proc Natl Acad Sci. 2008; 105: 16831–16836. https://doi.org/10.1073/pnas.0808687105 PMID: 18854416

8. Yuan L, Song X, Zhang L, Yu Y, Liang Z, Lei Y, et al. The transcriptional repressors VAL1 and VAL2 recruit PRC2 for genome-wide Polycomb silencing in Arabidopsis. Nucleic Acids Res. 2021; 49: 98–113. https://doi.org/10.1093/nar/gkaa1129 PMID: 33270882

9. Qüesta JI, Song J, Geraldo N, An H, Dean C. Arabidopsis transcriptional repressor VAL1 triggers Polycomb silencing at FLC during vernalization. Science (80-). 2016; 353: 485–488. https://doi.org/10.1126/science.aaf7354 PMID: 27471304

10. Bieluszewski T, Xiao J, Yang Y, Wagner D. PRC2 activity, recruitment, and silencing: a comparative perspective. Trends Plant Sci. 2021; 26: 1186–1198. https://doi.org/10.1016/j.tplants.2021.06.006 PMID: 34294542

11. Sung S, Schmitz RJ, Amasino RM. A PHD finger protein involved in both the vernalization and photoperiod pathways in Arabidopsis. Genes Dev. 2006; 20: 3244–3248. https://doi.org/10.1101/gad.1493306 PMID: 17114575

12. Amasino RM, Sung S. Vernalization in Arabidopsis thaliana is mediated by the PHD finger protein VIN3. Nature. 2004; 427: 159–164. https://doi.org/10.1038/nature02195 PMID: 14712276

13. Greb T, Dean C, Mylne JS, Crevillen P, Geraldo N, An H, et al. The PHD finger protein VRN5 functions in the epigenetic silencing of Arabidopsis FLC. Curr Biol. 2007; 17: 73–78. https://doi.org/10.1016/j.cub.2006.11.052 PMID: 17174094

14. Kim DH, Sung S. Coordination of the vernalization response through a VIN3 and FLC gene family regulatory network in Arabidopsis. Plant Cell. 2013; 25: 454–469. https://doi.org/10.1105/tpc.112.104760 PMID: 23417034

15. Kim D-H, Sung S. The Plant Homeo Domain finger protein, VIN3-LIKE 2, is necessary for photoperiod-mediated epigenetic regulation of the floral repressor, MAF5. Proc Natl Acad Sci. 2010; 107: 17029–17034. https://doi.org/10.1073/pnas.1010834107 PMID: 20837520

16. Zhao SQ, Hu J, Guo LB, Qian Q, Xue HW. Rice leaf inclination2, a VIN3-like protein, regulates leaf angle through modulating cell division of the collar. Cell Res. 2010; 20: 935–947. https://doi.org/10.1038/cr.2010.109 PMID: 20644566

17. Yoon H, Yang J, Liang W, Zhang D, An G. OsVIL2 Regulates Spikelet Development by Controlling Regulatory Genes in Oryza sativa. Front Plant Sci. 2018; 9: 1–12. https://doi.org/10.3389/fpls.2018.00001 PMID: 29410674

18. Yang J, Lee S, Hang R, Kim SR, Lee YS, Cao X, et al. OsVIL2 functions with PRC2 to induce flowering by repressing O s LFL 1 in rice. Plant J. 2013; 73: 566–578. https://doi.org/10.1111/tpj.12057 PMID: 23083333

19. Yang J, Cho LH, Yoon J, Yoon H, Wai AH, Hong WJ, et al. Chromatin interacting factor OsVIL2 increases biomass and rice grain yield. Plant Biotechnol J. 2019; 17: 178–187. https://doi.org/10.1111/pbi.12956 PMID: 29851259

20. Wang J, Hu J, Qian Q, Xue HW. LC2 and OsVIL2 promote rice flowering by photoperoid-induced epigenetic silencing of OsLF. Mol Plant. 2013; 6: 514–527. https://doi.org/10.1093/mp/sss096 PMID: 22973062

21. An Y, Guo Y, Liu C, An H. BdVIL4 regulates flowering time and branching through repressing miR156 in ambient temperature dependent way in Brachypodium distachyon. Plant Physiol Biochem. 2015; 89: 92–99. https://doi.org/10.1016/j.plaphy.2015.02.013 PMID: 25728135

22. Jeong HJ, Yang J, Cho LH, An G. OsVIL1 controls flowering time in rice by suppressing OsLF under short days and by inducing Ghd7 under long days. Plant Cell Rep. 2016; 35: 905–920. https://doi.org/10.1007/s00299-015-1931-5 PMID: 26795142

23. Fu D, Dunbar M, Dubcovsky J. Wheat VIN3-like PHD finger genes are up-regulated by vernalization. Mol Genet Genomics. 2007; 277: 301–313. https://doi.org/10.1007/s00438-006-0189-6 PMID: 17123111

24. Almutairi ZM, Sadder MT. Cloning and expression profiling polycomb gene VERNALIZATION INSENSITIVE 3 in tomato. Biol Plant. 2014; 58: 419–426. https://doi.org/10.1007/s10535-014-0421-x

25. Mohan V, Borovsky Y, Kamara I, Zemach H, Paran I. CaVIL1, a plant homeodomain gene that promotes flowering in pepper. Theor Appl Genet. 2018; 131: 2639–2649. https://doi.org/10.1007/s00122-018-3179-2 PMID: 30194521

26. Yoon J, Cho L-HH, Lee S, Pasriga R, Tun W, Yang J, et al. Chromatin Interacting Factor OsVIL2 Is Required for Outgrowth of Axillary Buds in Rice. Mol Cells. 2019; 42: 858–868. https://doi.org/10.14348/molcells.2019.0141 PMID: 31771322

27. Bar M, Ori N. Compound leaf development in model plant species. Curr Opin Plant Biol. 2015; 23: 61–69. https://doi.org/10.1016/j.pbi.2014.10.007 PMID: 25449728

28. Hagemann W, Gleissberg S. Organogenetic capacity of leaves: the significance of marginal blastozones in angiosperms. Plant Syst Evol. 1996; 199: 121–152.

29. Shleizer-Burko S, Burko Y, Ben-Herzel O, Ori N. Dynamic growth program regulated by LANCEOLATE enables flexible leaf patterning. Development. 2011; 138: 695–704. dev.056770 [pii] https://doi.org/10.1242/dev.056770 PMID: 21228002

30. Blein T, Hasson A, Laufs P. Leaf development: what it needs to be complex. Curr Opin Plant Biol. 2010; 13: 75–82. S1369-5266(09)00141-1 [pii] https://doi.org/10.1016/j.pbi.2009.09.017 PMID: 19853496

31. Israeli A, Ben-Herzel O, Burko Y, Shwartz I, Ben-Gera H, Harpaz-Saad S, et al. Coordination of differentiation rate and local patterning in compound-leaf development. New Phytol. 2021; 229: 3558–3572. https://doi.org/10.1111/nph.17124 PMID: 33259078

32. Israeli A, Burko Y, Shleizer-Burko S, Zelnik ID, Sela N, Hajirezaei MR, et al. Coordinating the morphogenesis-differentiation balance by tweaking the cytokinin-gibberellin equilibrium. PLOS Genet. 2021; 17: e1009537. https://doi.org/10.1371/journal.pgen.1009537 PMID: 33901177

33. Kierzkowski D, Runions A, Vuolo F, Huijser P, Smith RS, Tsiantis M, et al. Article A Growth-Based Framework for Leaf Shape Development and Diversity Article A Growth-Based Framework for Leaf Shape Development and Diversity. Cell. 2019; 177: 1405–1418. https://doi.org/10.1016/j.cell.2019.05.011 PMID: 31130379

34. Koenig D, Bayer E, Kang J, Kuhlemeier C, Sinha N. Auxin patterns Solanum lycopersicum leaf morphogenesis. Development. 2009; 136: 2997–3006. https://doi.org/10.1242/dev.033811 PMID: 19666826

35. Ben-Gera H, Ori N. Auxin and LANCEOLATE affect leaf shape in tomato via different developmental processes. Plant Signal Behav. 2012;7. https://doi.org/10.4161/psb.7.1.18353 PMID: 22301957

36. Barkoulas M, Hay A, Kougioumoutzi E, Tsiantis M. A developmental framework for dissected leaf formation in the Arabidopsis relative Cardamine hirsuta. NatGenet. 2008; 40: 1136–1141. https://doi.org/10.1038/ng.189 PMID: 19165928

37. Bilsborough GD, Runions A, Barkoulas M, Jenkins HW, Hasson A, Galinha C, et al. Model for the regulation of Arabidopsis thaliana leaf margin development. Proc Natl Acad Sci U S A. 2011; 108: 3424–3429. 1015162108 [pii] https://doi.org/10.1073/pnas.1015162108 PMID: 21300866

38. Xiong Y, Jiao Y. The Diverse Roles of Auxin in Regulating. Plants. 2019; 8: 1–14. https://doi.org/10.3390/plants8070243 PMID: 31340506

39. Israeli A, Capua Y, Shwartz I, Bar M, Efroni I, Israeli A, et al. Multiple Auxin-Response Regulators Enable Stability and Variability in Leaf Development Article Multiple Auxin-Response Regulators Enable Stability and Variability in Leaf Development. Curr Biol. 2019; 29: 1746–1759.e5. https://doi.org/10.1016/j.cub.2019.04.047 PMID: 31104930

40. Ben-Gera H, Dafna A, Alvarez JPP, Bar M, Mauerer M, Ori N. Auxin-mediated lamina growth in tomato leaves is restricted by two parallel mechanisms. Plant J. 2016; 86: 443–457. https://doi.org/10.1111/tpj.13188 PMID: 27121172

41. Berger Y, Harpaz-Saad S, Brand A, Melnik H, Sirding N, Alvarez JPP, et al. The NAC-domain transcription factor GOBLET specifies leaflet boundaries in compound tomato leaves. Development. 2009; 136: 823–832. https://doi.org/10.1242/dev.031625 PMID: 19176589

42. Ben-Gera H, Shwartz I, Shao M-RR, Shani E, Estelle M, Ori N. ENTIRE and GOBLET promote leaflet development in tomato by modulating auxin response. Plant J. 2012; 70: 903–915. https://doi.org/10.1111/j.1365-313X.2012.04939.x PMID: 22332729

43. Wang H, Jones B, Li Z, Frasse P, Delalande C, Regad F, et al. The tomato Aux/IAA transcription factor IAA9 is involved in fruit development and leaf morphogenesis. Plant Cell. 2005; 17: 2676–2692. https://doi.org/10.1105/tpc.105.033415 PMID: 16126837

44. Menda N, Semel Y, Peled D, Eshed Y, Zamir D. In silico screening of a saturated mutation library of tomato. Plant J. 2004; 38: 861–872. https://doi.org/10.1111/j.1365-313X.2004.02088.x PMID: 15144386

45. Dengler NG, Tsukaya H. Leaf morphogenesis in dicotyledons: current issues. Int J Plant Sci. 2001; 162: 459–464.

46. Kaplan DR. Fundamental concepts of leaf morphology and morphogenesis: a contribution to the interpretation of molecular genetic mutants. Int JPlant Sci. 2001; 162: 465–474.

47. Ori N, Cohen ARR, Etzioni A, Brand A, Yanai O, Shleizer S, et al. Regulation of LANCEOLATE by miR319 is required for compound-leaf development in tomato. Nat Genet. 2007; 39: 787–791. https://doi.org/10.1038/ng2036 PMID: 17486095

48. Bar M, Israeli A, Levy M, Gera HB, Jiménez-Gómez JM, Kouril S, et al. CLAUSA is a MYB transcription factor that promotes leaf differentiation by attenuating cytokinin signaling. Plant Cell. 2016; 28: 1602–1615. https://doi.org/10.1105/tpc.16.00211 PMID: 27385816

49. Avivi Y, Lev-Yadun S, Morozova N, Libs L, Williams L, Zhao J, et al. Clausa, a tomato mutant with a wide range of phenotypic perturbations, displays a cell type-dependent expression of the homeobox gene LeT6/TKn21. Plant Physiol. 2000; 124: 541–551. https://doi.org/10.1104/pp.124.2.541 PMID: 11027705

50. Jasinski S, Kaur H, Tattersall A, Tsiantis M. Negative regulation of KNOX expression in tomato leaves. Planta. 2007; 226: 1255–1263. https://doi.org/10.1007/s00425-007-0572-5 PMID: 17628827

51. Bar M, Ben-Herzel O, Kohay H, Shtein I, Ori N. CLAUSA restricts tomato leaf morphogenesis and GOBLET expression. Plant J. 2015; 83: 888–902. https://doi.org/10.1111/tpj.12936 PMID: 26189897

52. Shani E, Burko Y, Lilach B-Y, Berger Y, Amsellem Z, Goldshmidt A, et al. Stage-specific regulation of Solanum lycopersicum leaf maturation by class 1 KNOTTED1-LIKE HOMEOBOX proteins. Plant Cell. 2009; 21: 3078–3092. tpc.109.068148 [pii] https://doi.org/10.1105/tpc.109.068148 PMID: 19820191

53. Bolger A, Scossa F, Bolger ME, Lanz C, Maumus F, Tohge T, et al. The genome of the stress-tolerant wild tomato species Solanum pennellii. Nat Genet. 2014; 46: 1034–1038. https://doi.org/10.1038/ng.3046 PMID: 25064008

54. Kumar S, Stecher G, Li M, Knyaz C, Tamura K. MEGA X: Molecular Evolutionary Genetics Analysis across Computing Platforms. Mol Biol Evol. 2018; 35: 1547–1549. https://doi.org/10.1093/molbev/msy096 PMID: 29722887

55. Jones DT, Taylor WR, Thornton JM. The rapid generation of mutation data matrices from protein sequences. Comput Appl Biosci. 1992; 8: 275–282. https://doi.org/10.1093/bioinformatics/8.3.275 PMID: 1633570

56. Moore I, Galweiler L, Grosskopf D, Schell J, Palme K. A transcription activation system for regulated gene expression in transgenic plants. Proc Natl Acad Sci USA. 1998; 95: 376–381. https://doi.org/10.1073/pnas.95.1.376 PMID: 9419383

57. Brukhin V, Hernould M, Gonzalez N, Chevalier C, Mouras A. Flower development schedule in tomato Lycopersicon esculentum cv. sweet cherry. Sex Plant Reprod. 2003; 15: 311–320. https://doi.org/10.1007/s00497-003-0167-7

58. Hileman LC, Sundstrom JF, Litt A, Chen M, Shumba T, Irish VF. Molecular and Phylogenetic Analyses of the MADS-Box Gene Family in Tomato. Mol Biol Evol. 2006; 23: 2245–2258. https://doi.org/10.1093/molbev/msl095 PMID: 16926244

59. Tian T, Liu Y, Yan H, You Q, Yi X, Du Z, et al. agriGO v2.0: a GO analysis toolkit for the agricultural community, 2017 update. Nucleic Acids Res. 2017; 45: W122–W129. https://doi.org/10.1093/nar/gkx382 PMID: 28472432

60. Mouriz A, López-González L, Jarillo JA, Piñeiro M. PHDs govern plant development. Plant Signal Behav. 2015; 10: e993253. https://doi.org/10.4161/15592324.2014.993253 PMID: 26156103

61. Zhao Y, Antoniou-Kourounioti RL, Calder G, Dean C, Howard M. Temperature-dependent growth contributes to long-term cold sensing. Nature. 2020; 583: 825–829. https://doi.org/10.1038/s41586-020-2485-4 PMID: 32669706

62. Shalit A, Rozman A, Goldshmidt A, Alvarez JP, Bowman JL, Eshed Y, et al. The flowering hormone florigen functions as a general systemic regulator of growth and termination. Proc Natl Acad Sci U S A. 2009; 106: 8392–8397. https://doi.org/10.1073/pnas.0810810106 PMID: 19416824

63. Shalit-Kaneh A, Eviatar-Ribak T, Horev G, Suss N, Aloni R, Eshed Y, et al. The flowering hormone florigen accelerates secondary cell wall biogenesis to harmonize vascular maturation with reproductive development. Proc Natl Acad Sci. 2019; 116: 16127–16136. https://doi.org/10.1073/pnas.1906405116 PMID: 31324744

64. Lifschitz E, Ayre BG, Eshed Y. Florigen and anti-florigen â€"a systemic mechanism for coordinating growth and termination in flowering plants. Front Plant Sci. 2014; 5: 1–14. https://doi.org/10.3389/fpls.2014.00465 PMID: 25278944

65. Navarro C, Abelenda JA, Cruz-Oró E, Cuéllar CA, Tamaki S, Silva J, et al. Control of flowering and storage organ formation in potato by FLOWERING LOCUS T. Nature. 2011; 478: 119–122. https://doi.org/10.1038/nature10431 PMID: 21947007

66. Cartolano M, Pieper B, Lempe J, Tattersall A, Huijser P, Tresch A, et al. Heterochrony underpins natural variation in Cardamine hirsuta leaf form. Proc Natl Acad Sci U S A. 2015; 112: 10539–10544. https://doi.org/10.1073/pnas.1419791112 PMID: 26243877

67. Burko Y, Shleizer-Burko S, Yanai O, Shwartz I, Zelnik ID, Jacob-Hirsch J, et al. A role for APETALA1/fruitfull transcription factors in tomato leaf development. Plant Cell. 2013; 25: 2070–2083. https://doi.org/10.1105/tpc.113.113035 PMID: 23771895

68. Silva GFF, Silva EM, Correa JPO, Vicente MH, Jiang N, Notini MM, et al. Tomato floral induction and flower development are orchestrated by the interplay between gibberellin and two unrelated microRNA-controlled modules. New Phytol. 2019; 221: 1328–1344. https://doi.org/10.1111/nph.15492 PMID: 30238569

69. Goodrich J, Puangsomlee P, Martin M, Long D, Meyerowitz EM, Coupland G. A Polycomb-group gene regulates homeotic gene expression in Arabidopsis. Nature. 1997; 386: 44–51. https://doi.org/10.1038/386044a0 PMID: 9052779

70. Wang J, Hu J, Qian Q, Xue H-W. LC2 and OsVIL2 promote rice flowering by photoperoid-induced epigenetic silencing of OsLF Mol Plant. 2013 Mar; 6(2):514–27. https://doi.org/10.1093/mp/sss096 Epub 2012 Sep 12.

71. Weber CM, Hafner A, Kirkland JG, Braun SMG, Stanton BZ, Boettiger AN, et al. mSWI/SNF promotes Polycomb repression both directly and through genome-wide redistribution. Nat Struct Mol Biol. 2021; 28: 501–511. https://doi.org/10.1038/s41594-021-00604-7 PMID: 34117481

72. Shwartz I, Levy M, Ori N, Bar M. Hormones in tomato leaf development. Dev Biol. 2016;419. https://doi.org/10.1016/j.ydbio.2016.06.023 PMID: 27339291

73. Kim D, Pertea G, Trapnell C, Pimentel H, Kelley R, Salzberg SL. TopHat2: Accurate alignment of transcriptomes in the presence of insertions, deletions and gene fusions. Genome Biol. 2013; 14: R36. https://doi.org/10.1186/gb-2013-14-4-r36 PMID: 23618408

74. Depristo MA, Banks E, Poplin R, Garimella KV, Maguire JR, Hartl C, et al. A framework for variation discovery and genotyping using next-generation DNA sequencing data. Nat Genet. 2011; 43: 491–501. https://doi.org/10.1038/ng.806 PMID: 21478889

75. Wang K, Li M, Hakonarson H. ANNOVAR: functional annotation of genetic variants from high-throughput sequencing data. Nucleic Acids Res. 2010; 38: e164–e164. https://doi.org/10.1093/nar/gkq603 PMID: 20601685

76. Kurihara D, Mizuta Y, Sato Y, Higashiyama T. ClearSee: A rapid optical clearing reagent for whole-plant fluorescence imaging. Development. 2015; 142: 4168–4179. https://doi.org/10.1242/dev.127613 PMID: 26493404

77. Exposito-Rodriguez M, Borges AA, Borges-Perez A, Perez JA, Expósito-Rodríguez M, Borges AA, et al. Selection of internal control genes for quantitative real-time RT-PCR studies during tomato development process. BMC Plant Biol. 2008; 8: 131. 1471-2229-8-131 [pii] https://doi.org/10.1186/1471-2229-8-131 PMID: 19102748

78. Shani E, Ben-Gera H, Shleizer-Burko S, Burko Y, Weiss D, Ori N. Cytokinin regulates compound leaf development in tomato c w. Plant Cell. 2010;22. https://doi.org/10.1105/tpc.110.078253 PMID: 20959562

79. Gendrel AV, Lippman Z, Martienssen R, Colot V. Profiling histone modification patterns in plants using genomic tiling microarrays. Nat Methods. 2005; 2: 213–218. https://doi.org/10.1038/nmeth0305-213 PMID: 16163802

80. Langmead B, Salzberg SL. Fast gapped-read alignment with Bowtie 2. Nat Methods. 2012; 9: 357–359. https://doi.org/10.1038/nmeth.1923 PMID: 22388286

81. Li H, Handsaker B, Wysoker A, Fennell T, Ruan J, Homer N, et al. The Sequence Alignment/Map format and SAMtools. Bioinformatics. 2009; 25: 2078–2079. https://doi.org/10.1093/bioinformatics/btp352 PMID: 19505943

82. Heinz S, Benner C, Spann N, Bertolino E, Lin YC, Laslo P, et al. Simple Combinations of Lineage-Determining Transcription Factors Prime cis-Regulatory Elements Required for Macrophage and B Cell Identities. Mol Cell. 2010; 38: 576–589. https://doi.org/10.1016/j.molcel.2010.05.004 PMID: 20513432

83. Ramírez F, Ryan DP, Grüning B, Bhardwaj V, Kilpert F, Richter AS, et al. deepTools2: a next generation web server for deep-sequencing data analysis. Nucleic Acids Res. 2016; 44: W160–W165. https://doi.org/10.1093/nar/gkw257 PMID: 27079975

84. Dobin A, Davis CA, Schlesinger F, Drenkow J, Zaleski C, Jha S, et al. STAR: ultrafast universal RNA-seq aligner. Bioinformatics. 2013; 29: 15–21. https://doi.org/10.1093/bioinformatics/bts635 PMID: 23104886

85. Love MI, Huber W, Anders S. Moderated estimation of fold change and dispersion for RNA-seq data with DESeq2. Genome Biol. 2014; 15: 1–21. https://doi.org/10.1186/s13059-014-0550-8 PMID: 25516281

86. Kim SK, Lund J, Kiraly M, Duke K, Jiang M, Stuart JM, et al. A gene expression map for Caenorhabditis elegans. Science (80-). 2001; 293: 2087–2092. https://doi.org/10.1126/science.1061603 PMID: 11557892